



UNIVERSITY OF LEEDS

This is a repository copy of *Outcrop architecture of a fluvio-lacustrine succession: Upper Triassic Yanchang Formation, Ordos Basin, China*.

White Rose Research Online URL for this paper:
<http://eprints.whiterose.ac.uk/89893/>

Version: Accepted Version

Article:

Zhao, J, Mountney, NP, Liu, C et al. (2 more authors) (2015) Outcrop architecture of a fluvio-lacustrine succession: Upper Triassic Yanchang Formation, Ordos Basin, China. *Marine and Petroleum Geology*, 68 (A). 394 - 413. ISSN 0264-8172

<https://doi.org/10.1016/j.marpetgeo.2015.09.001>

© 2015, Elsevier. Licensed under the Creative Commons Attribution-NonCommercial-NoDerivatives 4.0 International
<http://creativecommons.org/licenses/by-nc-nd/4.0/>

Reuse

Unless indicated otherwise, fulltext items are protected by copyright with all rights reserved. The copyright exception in section 29 of the Copyright, Designs and Patents Act 1988 allows the making of a single copy solely for the purpose of non-commercial research or private study within the limits of fair dealing. The publisher or other rights-holder may allow further reproduction and re-use of this version - refer to the White Rose Research Online record for this item. Where records identify the publisher as the copyright holder, users can verify any specific terms of use on the publisher's website.

Takedown

If you consider content in White Rose Research Online to be in breach of UK law, please notify us by emailing eprints@whiterose.ac.uk including the URL of the record and the reason for the withdrawal request.



eprints@whiterose.ac.uk
<https://eprints.whiterose.ac.uk/>

Outcrop Architecture of a Fluvio-Lacustrine Succession: Upper Triassic Yanchang Formation, Ordos Basin, China

Junfeng Zhao^{1,2,3}, Nigel P. Mountney³, Chiyang Liu^{1,2}, Hongjun Qu^{1,2}, Jinyan Lin^{1,2}

1 State Key Laboratory of Continental Dynamics, Northwest University, Xi'an, China. zjf@nwu.edu.cn

2 Department of Geology, Northwest University, Xi'an, China.

3 Fluvial & Eolian Research Group, School of Earth and Environment, University of Leeds, Leeds, UK. n.p.mountney@leeds.ac.uk

Abstract: Although several studies have considered the sedimentary facies of the Upper Triassic Yanchang Formation in terms of their hydrocarbon potential in the petroliferous Ordos Basin, such studies have mostly interpreted subsurface data and few have systematically examined the detailed outcrop-based anatomy of this succession. This study characterizes a series of well-exposed outcrop sections along an 80-km-long E-W oriented series of road cuttings in the southeast Ordos Basin to reconstruct the sedimentary architecture of a fluvio-lacustrine succession and determine the principal controls that governed the style of accumulation and preservation. The Yanchang Formation is divided into 10 depositional units – Chang 10 (base) to Chang 1 (top) – that record the sedimentary evolution of a series of large scale fluvial systems that constructed delta-front and pro-delta bodies as they entered a large, interior-draining lake. Deposits of the Chang 10 to 1 units record 4 major lacustrine transgressive events during the late Triassic in the form of 10 to 20 m-thick oil-shale-prone intervals. Sandstone-prone facies associations mainly accumulated in fluvial channel, delta-plain and upper delta-front environments; these units record 4 major progradational events. The uppermost Chang 1 interval is characterized by laterally accreted fluvial sandstone bodies overlain by claystone overbank deposits with thin interbedded coal seams and records late-stage filling of the lacustrine basin. Detailed analysis of the internal architectures of the delta-front bodies records the mechanism of growth of a large-scale, shallow-water delta succession. However, significant differences are identified in the development of this lacustrine delta compared to that of more commonly recognized marine shelf-edge delta systems. Lacustrine subaqueous distributary channels have 3 to 15 m-thick sandstone fills and

are more abundant and better developed than their marine counterparts: such channelized bodies are highly elongate and many can be traced several kilometres. Such bodies can be shown to be commonly associated with thin-bedded mouth-bar and subaqueous interdistributary-bay deposition. Overall, the Yanchang Formation is characterized by 4 major transgressive-regressive cycles, the development of which was controlled by a combination of changes in the rate of tectonic subsidence, the rate of sediment delivery from the basin margin hinterland and climate – factors that were themselves influenced by intracontinental growth of the neighbouring Qinling Orogen.

Key words: Fluvio-lacustrine succession, meandering river, shallow-water delta, architectural elements, outcrop, Yanchang Formation, Ordos Basin.

1 Introduction

Fluvio-lacustrine depositional systems are commonly recognized palaeoenvironments that have been interpreted from a wide variety of ancient preserved successions. Several aspects of the sedimentology of fluvio-lacustrine depositional systems have been the focus of considerable attention: (i) the establishment of criteria for the recognition of the preserved expression of different types of river systems at their point of terminus into lakes (e.g. [Jiao et al, 2005](#); [Eric, 2007](#); [Dill et al., 2006](#); [Nichols and Fisher, 2007](#); [Ghinassi et al, 2009](#); [Weissmann et al, 2010](#)); (ii) the impact of terrestrial vegetation on fluvio-lacustrine sedimentation ([Davies and Gibling, 2010a,b](#)); (iii) the role of gravity-current and sandy debris-flow processes in governing sediment distribution to deep or off-shore lake areas ([Shanmugam, 2000](#); [Bouma, 2000](#)); (iv) the development of objective criteria for the identification of lacustrine deltas ([Morris et al, 1991](#); [Olsen, 1995](#); [Carroll and Bohacs, 1999](#); [Tanner and Lucas, 2010](#); [Olariu et al., 2010](#)); (v) the development of sequence stratigraphic models for fluvio-lacustrine successions ([Keighley et al, 2003](#); [Keighley and Flint, 2008](#)); (vi) quantitative studies of the sedimentary architecture of fluvio-lacustrine successions ([Morris and Richmond, 1992](#); [Taylor and Ritts, 2004](#); [Colombera et al, 2012, 2013](#)).

Fluvio-lacustrine successions are widely developed in numerous Meso-Cenozoic

sedimentary basins in China, from which more than 90% of domestic Chinese liquid hydrocarbon production originates (Xu et al, 1998; Zhao et al, 2010; Yu and Li, 2009). Thus, gaining an improved understanding of the internal anatomy and the external controls on the style of stacking of larger scale bodies in such successions has applied importance. Furthermore, demonstrating how and why the preserved sedimentary architectures of fluvio-lacustrine deltaic successions differ from those of more commonly recognized marine-influenced deltaic successions is important for establishing criteria for the recognition of such bodies and for wider palaeogeographic reconstruction. Previous studies of fluvio-lacustrine successions from Chinese sedimentary basins have been based primarily on analysis of subsurface borehole, well-log and seismic data sets (e.g. Zou et al, 2012; Yu et al, 2010); relatively few studies have focused on detailed outcrop-based sedimentary anatomy (Jiao et al, 1995, 2005; Qi et al, 2009; Xin et al, 1997; Wang, 2001; Yu et al, 2013; Zou et al, 2010; Zou et al, 2012).

The Ordos Basin is the second largest petroliferous basin in China; both the rate of hydrocarbon production and the estimate of ultimate recoverable reserves have increased in recent years (Yang et al, 2005; Xiao et al, 2005; Liu et al, 2008; Fig. 1). Petroleum resources of the basin are mainly accumulated in fluvio-lacustrine deposits of the Upper Triassic Yanchang Formation (Deng et al, 2011). Although a small number of previous outcrop-based studies of the Yanchang Formation have focused on the characterization of the sedimentology and the recognition of architectural elements (Jiao et al, 1995; Zou et al, 2010; Wang et al, 2004; Zhang et al, 2006; Zhao et al, 2014), these have primarily focused on reservoir property surveys, geological modelling and the establishment of a regional sequence stratigraphic framework to assist in hydrocarbon exploration and field development at a regional scale.

The aim of this study is to document the detailed internal anatomy of a well-exposed fluvio-lacustrine succession and to establish the autogenic and allogenic controls that governed the style of accumulation and preservation of the succession. Specific objectives are as follows: (i) to document the typical lithofacies types present in the fluvio-lacustrine succession represented by the various intervals of the Yanchang Formation; (ii) to document the lithofacies composition and internal architectural arrangement of elements that comprise the fluvial, delta front and shallow-water lacustrine components of the system and their

inter-relationships; (iii) to develop a model with which to account for the pattern of sedimentation recorded in the Yanchang Formation and to relate this to long-term and large-scale development of the intracratonic Ordos Basin; (iv) to provide a detailed outcrop-based case study that can be used as an analog for subsurface reservoir characterization; (v) to contrast the sedimentology of a shallow-water fluvio-lacustrine deltaic succession with that of more commonly recognized marine-influenced deltaic successions.

2 Geological setting

The Ordos Basin is a large scale residual Mesozoic intracratonic down-warped basin located in the western part of the North China Craton (NCC). It developed during the Middle Triassic to Early Cretaceous in a position superimposed upon the larger, Palaeozoic North China Basin (Liu et al, 2008). The Ordos Basin originally covered an area of ~ 5 to 6×10^5 km². However, the region has been affected by intensive post-depositional uplift and reformation in the eastern NCC since the Late Cretaceous, meaning that the eastern part of the original Ordos Basin has been significantly eroded (Liu et al, 2008; Zou et al, 2010). The present-day residual western part of the basin covers an area of 2.5×10^5 km². The sedimentary fill of the Ordos Basin is characterized predominantly by fluvio-lacustrine successions of middle Triassic to middle Jurassic age, whereas alternating fluvial and aeolian successions accumulated in the early Cretaceous (Liu et al, 2008; Zhao et al, 2009; Fig. 2).

The 800 to 1500 m-thick Upper Triassic Yanchang Formation is an important petroleum exploration interval in the Ordos Basin, with a general trend of thickening southward. The area between Yanchi, Wuqi and Fuxian (Fig. 3) represents a northwest-southeast oriented depocentre that developed during the late Triassic. A series of meandering fluvial channel systems occupied a broad delta plain in the north-eastern part of the basin during deposition of Yanchang Formation, whereas a series of braided river-deltaic systems and fan deltaic systems developed in the south-western part of the basin (Zou et al, 2010; Fig. 3). The provenance of sediment delivered to the basin was the Palaeo-Yin Mountain to the north and the Qinling orogenic belt to the south of the Ordos Basin (Zou et al, 2010; Yu et al, 2013; Fig. 3).

The entire Yanchang Formation is divided into ten oil-prone layers or lithological

intervals named Chang 10 (base) to Chang 1 (top), the boundaries of which are defined by the occurrence of laterally persistent marker layers (K₀-K₉), including syn-sedimentary tuff beds and oil-shale units developed within the Yanchang Formation, each of which has a distinct response on wire-line logs, making them useful for subsurface correlation. Within the Yanchang Formation, the Chang 7 interval is the main source rock, whereas the sand-prone Chang 8, 6, 5 and 4 intervals serve as the major reservoirs (Li et al, 2009; Deng et al, 2011). In recent years, the lowermost Chang 10 and 9 intervals have also been identified as important hydrocarbon reservoir and source units, respectively (Wanyan et al, 2011).

The studied sections discussed herein are located in the south-eastern part of the Ordos Basin along the Xianchuan River and the Luo River (Fig. 1) where the Yanchang Formation is well exposed in a series of laterally extensive road cuttings and natural outcrops. The effects of post-depositional inversion of the basin are relatively mild in this region and the Mesozoic strata are essentially non-deformed such that the succession is nearly flat-lying and not disrupted by faulting.

3 Methodology

As an important oil and gas producing area, tens of thousands of boreholes penetrate the Upper Triassic Yanchang Formation in the Ordos Basin, subsurface data from which have enabled the construction of a detailed lithofacies scheme to account for the principal depositional environments (Li et al, 2009; Deng et al, 2011; Yu et al, 2010). To complement these studies that utilized subsurface data, this study analyses an extensive outcrop-based dataset collected from two main areas: the Xianchuan River and the Luo River (Fig. 1). Representative outcrop sections of each interval (Chang 10 to Chang 1) have been studied in detail. Nine principal lithofacies types and 14 architectural element types are recognized (Tab. 1, 2). Lithofacies and architectural elements are classified and described using the a modified version of the popular classification scheme of Miall (1985; 1988a,b). Architectural elements refer to bodies of rock strata characterized by specific lithofacies assemblages, lithosome geometries, scales, and contact relationships (Miall 1988a,b). Sixteen 1D sedimentary graphic-log profiles have been measured, and these record data from a total of 280 m of measured section. Graphic profiles record lithology, grain size, sedimentary textures and

structures. Detailed sedimentary architectural relationships have been recorded on a series of 2D architectural panels that record a total of $3.7 \times 10^4 \text{ m}^2$ of outcropping stratigraphic sections in the form of scaled architectural drawings depicting bedding and bounding-surface relationships in a variety of orientations relative to inferred palaeoflow direction. Forty-three palaeocurrent measurements have been taken from planar and trough cross-bedding and asymmetric ripple marks and climbing-ripple cross-stratification. Outcrops of the Yanchang Formation in the study area have a persistent gentle westward tectonic dip of $<1^\circ$; as such each interval of the Yanchang Formation (Chang 10 to Chang 1) is exposed along an 80 km-long traverse from east to west.

4 Sedimentological Analysis of the Upper Triassic Yanchang Formation

4.1 Chang 10 interval

Description. The basal-most Chang 10 interval unconformably overlies purple-red mudstone of the Mid-Triassic Zhifang Formation (T_{2z}) (Fig. 2). The Chang 10 interval is 201-350 m thick and consists generally of salmon or grey-green medium to coarse grained quarto-feldspathic (arkosic) sandstone that occurs interbedded with silty mudstone. Sandstone layers are primarily developed at the base of the interval. The studied outcropping section lies at the contact interface with the underlying Zhifang Formation. The Chang 10 interval forms an upward-fining succession consisting predominantly of sandstone (Fig. 4). The middle and lower parts of the section are characterized by stacked, grey-green trough or tabular cross-bedded sandstone beds that are collectively 15 to 24 m thick and comprise two superposed lenticular sand bodies, each of which is $>450\text{m}$ in lateral extent (Fig. 4). The contact interface at the bottom of these sand bodies is a markedly undulating scour surface with up to 1.6 m of relief filled with mud pebbles and fossilized plant-stem debris (Fig. 4 – 4, 5, 6). The sand bodies are characterized by 0.3 to 1.2 m-thick sets of trough and tabular cross-bedding and parallel bedding (Fig. 4 – 1, 2, 7, 8), which record westerly-directed palaeoflow. Some of the beds have undergone syn-depositional deformation (Fig. 4 – 1, 2). The upper part of the Chang 10 interval is characterized by interbedded sandstone-mudstone layers arranged into thin cycles that are each 0.8 to 1.0 m thick.

Interpretation. The undulating scour surface and associated occurrence of mud pebble

clasts and fossilized plant-stem debris at the bottom base of the formation demonstrates the action of a scour and fill process. The two juxtaposed lenticular sand bodies, which internally comprise trough and tabular cross-bedded sets and parallel bedded sets of sandstone, arose via barform migration within a channelized setting (Walker, 1978; Friend, 1979). By contrast, the interbedded thin sandstone-mudstone layers in the upper part of the studied outcrop record repeated shifts between episodes of quiescence and the accumulation of floodplain sediments (FF), and a moderate energy regime that is typical in natural levee (LV) and crevasse spray (CS) settings (e.g. Allen, 1970). The westward palaeocurrent direction showed by cross bedding implies a provenance to the east (Fig. 4).

Previous interpretations of the Chang 10 interval have been based on regional subsurface well-log and core data supplemented by very limited outcrop data. Both alluvial-fan and fluvial palaeoenvironments were recognized, with deposits via fluvial stream-flow processes being dominant (Wanyan et al, 2011). Both braided and meandering fluvial styles have been inferred; deposits of the former occur predominantly in the central and western part of the basin, whereas deposits of the latter occur in the south-eastern part of the basin. The depocentre is possibly in the West Henan Province-East Qinling region, located to the southeast of the remnant Ordos Basin (Wanyan et al, 2011; Deng et al, 2011; Fig. 3).

4.2 Chang 9 interval

Description The Chang 9 interval is 80 to 100 m thick and is composed mainly of grey-green fine-grained sand, siltstone and grey-black or dark-grey mudstone, shale and oil shale; the sandstone proportion is about 35-45%, significantly less than in the Chang 10 interval. This interval comprise 4 to 6 upward-coarsening sedimentary cycles and each successive cycle contains progressively less sandstone and more mudstone (cf. Yu et al, 2010; Deng et al, 2011). The studied section records the middle part of the Chang 9 interval in west Qiulin town (Fig. 1d). Three upward-coarsening cycles are well exposed, each 10 to 15 m thick. Each cycle can be traced laterally along the road cutting for a distance of 1000 m (Figs. 5, 6). Each cycle has a lower part of dark-grey or grey-black horizontally laminated mudstone that parts readily to expose lamination surfaces upon which fine plant debris is evident. Overlying beds are thin grey-green siltstone and mudstone interbeds. The siltstone-prone

intervals are 0.3 to 0.5 m thick and contain syndepositional deformation structures including convolute bedding and water-escape features (Fig. 5 – 3, 5). The uppermost part of each cycle consists of 2.5 to 4.0 m-thick beds of fine sandstone with sharp but flat basal surfaces. Internally, the sandstone beds comprise trough and tabular cross-bedding (Fig. 5 – 1, 4) and in places these structures are overturned (Fig. 5 – 2). In the uppermost part of the Chang 9 interval, oil shale is present in the lower part of each cycle (Fig. 5 – 6, 7).

Interpretation. The assemblage of lithofacies and sedimentary structures and their arrangement into distinct upward-coarsening cycles records the repeated progradation of the distal parts of lobes of a subaqueous delta (cf. Zou et al, 2010; Olariu et al., 2010). The lowermost part of each cycle (dark grey to black mudstone with horizontal bedding) represents an environment below wave base in a pro-delta (PD) setting. The overlying thin grey-green siltstone-mudstone interbeds record weak scouring processes and wave action, which is typical of distal bar (DB) and mouth bar (MB) deposits (Turner et al, 2006). The sand-prone upper part of each cycle records in-channel deposition via weak hydrodynamic processes (Olariu et al., 2010). The presence of deformation structures implies localized relief on the accumulation surface and rapid accumulation, possibly in a subaqueous distributary channel (SCH) setting (Zou et al, 2010; Deng et al, 2011).

The Chang 9 interval records the initial development of the late Triassic Ordos lake basin in which a deltaic-lacustrine sedimentary succession accumulated, fed mostly from meandering fluvial systems to the northeast and the braided river deltaic systems in the southwest (cf. Yu et al, 2010; Deng et al, 2011: Fig. 3). The lake basin strikes NW-SE and gradually enlarged from the early to the late Chang 9 stage, when the semi-deep lake area covered an area of $\sim 4 \times 10^4$ km², and developed as an important source-rock interval – the “Lijiapan Shale” (also named K₁ marker bed), which is present in the upper Chang 9 interval (Fu et al, 2012; Fig. 2).

4.3 Chang 8 interval

Description. The Chang 8 interval is 75 to 90 m thick and consists of grey-green, medium- to fine-grained, lithic-feldspathic sandstone and feldspathic-lithic sandstone interbedded with grey-black carbonaceous mudstone. This interval is sand-rich sedimentary

succession that differs markedly from the underlying mud-prone Chang 9 interval. The studied section lies to the east of the county town of Yichuan (Fig. 1d) where a series of outcrops reveal the lower part of the Chang 8 interval. The sedimentary architecture is represented by an eastern and a western panel that are adjacent each other.

The eastern outcrop panel (Fig. 7) records a typical upward-coarsening succession. The bottom of the succession consists of dark-grey, horizontally laminated mudstone, overlain by grey-green mudstone with interbedded 30 to 50 mm-thick siltstone beds that preserve wave-rippled upper surfaces and internally reveal tabular sets with cross-lamination (Fig. 7 – 5, 6). Interference ripple marks are present in some cases. The thin-bedded siltstone bodies form thin sheet-like bodies that can be traced laterally for tens of metres. Medium-bedded sand bodies occur in the form of lenses that have sharp and flat bases but which have upper surfaces that are convex (Fig. 7 – 3). The middle and upper part of the recorded succession is represented by a juxtaposition of at least 4 lens-like, grey-green, fine-grained sand bodies, each 6 to 8 m thick. These bodies have mud-pebble and plant-stem lag deposits in their basal-most part (Fig. 7 – 1, 2), and are composed internally of sets of trough and tabular cross-bedding (Fig. 7 – 4).

The western outcrop panel also records an upward-coarsening succession but with a thicker developed sandstone association. The lower part consists of grey-green mudstone interbedded with thin- to medium-bedded siltstone. Interference ripple marks, small-scale ripple lamination and trough cross-bedding are common (Fig. 8 – 2, 3, 8). The middle and upper part of the western section is dominated by 3 laterally juxtaposed sand bodies (marked I, II, III in Fig. 8b). Erosional surfaces and associated mud-pebble and plant-stem lag deposits are common at the base and of each major sand body (Fig. 8 – 5) and trough and tabular cross-bedded sets are well developed in the upper parts of each.

Interpretation. The outcrop anatomy revealed by both architectural panels records an upward-coarsening, sandstone-prone feature in the lower part of Chang 8 interval. The upward transition from mudstone, to interbedded mudstone and siltstone is consistent with an upward-shallowing trend within a lacustrine setting (Olsen, 1995; Tanner et al, 2010). The lens-like sand bodies with their flat bases and convex upper surfaces are typical of mouth-bar deposits (Bhattacharya, 2006; Fig. 7 – 3). The offset lateral juxtaposition of the sand bodies is

indicative of multi-stage channel migration and lateral aggradation, with multiple episodes of cut, fill and migration. The assemblage of lithofacies with distinctive sedimentary structures, together with the sand-body morphology and architecture is collectively consistent with accumulation in a generally progradational subaqueous deltaic setting, within which pro-delta (PD) mudstones were overlain by delta-front distal bars (DB), mouth bars (MB), sand sheets (SB) and distributary bay (SDB) elements, which are in turn overlain by subaqueous distributary channel (SCH) deposits at the top of the succession (cf. [Coleman and Prior,1982](#); [Bhattacharya, 2006](#); [Ahmed et al, 2014](#)).

In the western panel, a juxtaposition of three upward-coarsening delta-front successions is recorded ([Fig. 9](#)) and these demonstrate a progressive westward outbuilding of the delta, which resulted in the preferential preservation of a notably sand-prone succession in the west of the study area. Although delta-front sedimentary successions are observed in both the Chang 9 and Chang 8 intervals, those in the Chang 8 interval are distinctly more sand prone and contain thicker subaqueous distributary channel elements (SCH), but lack widespread oil-shale deposits. This suggests that this episode of delta construction occurred during a period of intense fluvio-deltaic construction, possibly in response to heightened rates of sediment delivery or reduced lake level and contracted lake area.

Previous work based on regional studies ([Li et al, 2013](#)) argues that the base level of the overall Chang 8 interval underwent a rapid fall-and-rise cycle, such that a lower sub-interval recorded an episode of marked delta progradation, whereas an upper one recorded delta retrogradation. The outcrop succession of the Chang 8 interval studied here records the progradational phase: the lake basin shrank and the lake level dropped, enabling the delta to advance a considerable distance into the basin as recorded more regionally by the extensive presence of sand bodies. At this time, deep lacustrine deposition represented by dark shale or oil shale was restricted to the basin centre and did not cover a large area ([Yu et al,2010](#); [Deng et al, 2011](#)).

4.4 Chang 7 interval

Description. The Chang 7 interval is 100 to 120 m thick and consists of dark mudstone and oil shale interlayered with thin siltstone, fine sandstone or tuff. Two-to-five oil-shale

layers are developed in this interval with a cumulative thickness of 10 to 20 m; collectively this oil-shale prone unit is known as the "Zhangjiatan Shale", which forms the most important source rock for petroleum in the Ordos Basin (Yu et al, 2010; Deng et al, 2011).

The Chang 7 succession is exposed in outcrops 5 km west of the county town of Yichuan (Fig.1d) where an upward-coarsening succession is developed (Fig. 9). The lower part of the section consists of foliated black oil shale, which is more than 2 m thick; the base is not exposed (Fig. 11 – 1). Fossilized freshwater bivalve shells and fish scales are common. The oil shale is interbedded with 2 light-yellow tuff beds, each approximately 30 mm thick. The upper part of the section comprises grey-green, thick-bedded siltstone with wave-rippled upper bedding surfaces. Towards the top of the interval, units of medium-bedded trough cross-bedded sandstone are present, along with convolute bedding and symmetrical ripple marks.

Interpretation. The oil shale accumulated in a standing-water, anoxic environment, likely in a deep and offshore lacustrine setting (PD). The overlying thin siltstone with wave-ripple bedding and convolute bedding is indicative of deposition under the influence of wave and river-mouth interaction, and likely represents distal mouth bar (DB) and sheet-like bar (SB) deposits. The thick accumulation of oil shale and the presence of such deposits across the region (as recognized in well logs) demonstrate that the Chang 7 interval represents the episode of maximum lake extent (Li et al, 2009; Yu et al, 2010). In and around the Yijun region (Fig. 3), which located in the centre of the Chang 7 palaeo-lake basin (Fig. 3), a >15 m-thick succession of oil shale is exposed. The widespread tuffs interbeds demonstrate volcanic activity around the basin that was synchronous with sedimentation; they record the sedimentary response to volcanic processes associated with the Indosinian Orogeny in Qinling Mountain near the southern and south-western margins of the Ordos Basin (Qiu et al, 2013).

Lacustrine transgression is recorded by the Chang 7 interval; at this time lakes covered much of the central and southern parts of the Ordos Basin. Deep-water lacustrine deposits accumulated over an area of $\sim 9 \times 10^4$ km² (Deng et al, 2011). In these deep-water regions, fine-grained silt and mud deposits intercalated with fine-sand gravity-flow deposits accumulated. On the periphery of the lake basin, fluvio-deltaic deposits with a

retrogradational stacking arrangement have been recorded (Li et al., 2009; Yu et al, 2010).

4.5 Chang 6 interval

Description. The majority of the Chang 6 interval comprises grey-green sandstone interlayered with subordinate dark mudstone and thin tuff beds, which are collectively 110 to 130 m thick (Deng et al, 2011; Fig. 10). The Chang 6 interval along the studied Yichuan section is partly covered by Quaternary loess. However, from a relatively well-exposed section, 5 to 8 m-thick sandstone units have been studied and these take the form of laterally overlapping lenticular bodies, which internally comprise grey-green, fine sandstone with parallel and trough cross-bedding. Scour surfaces are present at the base of the sand bodies but generally have no appreciable erosional relief (Fig. 11 – 2), unlike the similar bodies in the Chang10 interval. These sand bodies are underlain by grey-black, horizontally laminated mudstone.

Interpretation. Coupled with observations from subsurface core data, outcrop-based lithofacies analysis suggests that the sand bodies in this interval are subaqueous distributary channel deposits (SCH), whereas underlying mudstone units are inter-distributary bay deposits (SDB). Compared to Chang 7, the Chang 6 interval is relatively sand prone and records deposition at a time of relatively low lake level that drove fluvio-deltaic progradation, as supported by well-log studies of regional extent, which confirm an episode of accumulation coincident with a relatively low lake level (Deng et al, 2011). A series of meandering fluvial and deltaic systems are recognized from subsurface data along the northeast flank of the basin (Yu et al, 2010; Deng et al, 2011; Fig. 3): these sand prone deposits form the principal hydrocarbon reservoir intervals for oil expelled from the underlying Chang 7 interval.

4.6 Chang 5 and 4 intervals

Description. The Chang 5 and 4 intervals are 80 to 90 m thick and comprise dark mudstone, carbonaceous mudstone and coal deposits interbedded with thin, grey-green siltstone and fine sandstone (Yu et al, 2010; Deng et al, 2011). The Chang 5 and 4 intervals are not well exposed along the Xianchuan River section (Fig. 12), though outcrops of limited lateral extent reveal 3 m-thick sand bodies with trough cross-bedding and parallel bedding.

Many fossilized plant stems (Fig. 11 – 4) are identified on the under-side of these sand bodies. The upper parts of the bodies comprise sandstone–mudstone interbeds with wave-rippled upper bedding surfaces and low-angle cross bedding (Fig. 11 – 3).

Interpretation. Deposits of the Chang 5 and 4 intervals examined here from outcrop are similar in character to those of Chang 6: they record the accumulation of delta-plain and delta-front sand bodies. Although not exposed, the central parts of the Chang 5 and 4 intervals, by contrast, record a minor lake transgression, as revealed by the development of offshore, shallow-water lacustrine deposits (Yu et al, 2010; Deng et al, 2011). The studied outcrop sections likely record near-shore, shallow-water lacustrine sand beach (SSB) and sand ridge (SSR) deposition. Regionally, Chang 5 and 4 intervals comprise thicker mudstone beds that are present over a wider area than equivalent deposits in the underlying Chang 6: this interval therefore likely records another episode of lake expansion.

4.7 Chang 3 and 2 intervals

Description. The Chang 3 and 2 intervals comprise light-grey and grey-green, massive, fine-medium-grained sandstone interbedded with dark-grey mudstone. These intervals are 90 to 110 m and 120 to 150 m thick, respectively. Both are sand-rich successions sharing the same features. Core and well-log data reveal that Chang 3 and 2 intervals are composed of 3-5 sedimentary cycles (Zou et al, 2010). To the west of Yingwang (Fig. 1d), a near-complete upward-coarsening succession is exposed (Fig. 13). A cross-section records three thick overlapping sand bodies, with weak scour surfaces present at the bottom of each. Fossilized plant stems and boulder-sized clay clasts are present directly above these surfaces (Fig. 11 – 5, 6, 7, 8). Internally, the sand bodies contain both trough and planar cross-bedding; thin-bedded mudstone interlayers are common.

Interpretation. The studied outcrop succession is most obviously interpreted as a series of laterally juxtaposed but offset subaqueous distributary channels (SCH), indicative of a lake regression episode late in the history of accumulation of the Yanchang Formation. Both the Chang 3 and Chang 2 intervals record episodes of lake contraction and associated fluvial and delta progradation. The presence of large, sand-filled channel bodies that have cut and scoured into underlying lacustrine mudstone deposits may have been generated by the

progressive draw-down of the lake level and an associated reduction in accommodation in lake-margin settings (cf. [Deng et al, 2011](#)).

4.8 Chang 1 interval

Description. The uppermost Chang 1 interval is characterized dominantly by grey-green mudstone interbedded with siltstone, fine sandstone and coal beds. As a consequence of tectonic uplift, which occurred after accumulation of the Yanchang Formation, the Chang 1 interval has been partly eroded and is incomplete; the preserved thickness 0 to 240 m ([Yu et al, 2010](#); [Deng et al, 2011](#)). On the west of the Xianchuan River section and south of the Luo River section, the upper Chang 1 Formation is well exposed (Fig.1). Along the Luo River section, outcrops of the Chang1 interval extend for ~2 km (Fig. 14). The lower 5 to 6 m is dominated by fine sandstone arranged into lenticular bodies (Fig. 14 – 1, 5). Wavy scour surfaces are identified at the base of some sand bodies, whereas parallel bedding, cross bedding and ripple lamination are present inside them (Fig. 14 – 2, 3). Ten mm-thick muddy interlayers are commonly present between the lenticular sand bodies (Fig. 14 – 5). The upper 5 to 7 m of the interval comprises mudstone interbedded with thin- or medium-bedded siltstone and coal seams. The siltstone deposits exhibit climbing-ripple stratification, asymmetrical ripple marks on upper bedding surfaces, fossilized plant stems and mud cracks (Fig. 14 – 6, 7, 8, 9).

Interpretation. The lenticular sand bodies present in the lower part of the interval are typical of channelized deposition with lateral accretion ([Bridge, 2006](#); [Miall, 2014](#)). Lithofacies and associated sedimentary structures in the upper part of the interval record the action of weak tractional currents that operated in a non-confined floodplain setting that was influenced by a sub-humid to humid climate ([Miall, 2006](#); [2014](#)). The fine-sandstone-dominated lower part and the mudstone- and coal-seam-dominated upper part compose a fining-upward vertical succession. Together they are indicative of a meandering fluvial succession ([Bridge, 2006](#); [Ethridge, 2011](#); [Miall, 2014](#)). Based on lithofacies associations, associated sedimentary structures and sand-body geometry, lateral accretion (LA), channel (CH), natural levee (LV), crevasse splay (CS), flood plain (FF) and swamp (SW) architectural elements are all identified (Fig. 14). Specifically, the laterally offset but

partly juxtaposed relationship of the sand bodies records laterally accretion from north to south across the studied outcrop.

Regionally, during accumulation of the Chang 1 interval, the palaeogeographic setting was characterized by a reduced rate of basin subsidence and deposition and development of a peneplain palaeo-topography (Liu et al, 2008; Deng et al, 2011). Widespread meandering river systems developed with broad floodplains; channel avulsion was likely common over the low-relief floodplain; vegetation development on the floodplain was extensive. During accumulation of the Chang 1 interval, the lake extent reduced substantially (Fig. 2), probably reflecting a reduced rate of basin subsidence at the end of the late Triassic. The basin at this time was largely filled by fluvial deposits.

5. Discussion

5.1 Controls on fluvio-lacustrine delta evolution

Results of facies characterization based on data from the studied outcrop sections reveal a sedimentary setting that conforms to the more general history of evolution of the Yanchang Formation revealed by data from tens of thousands of well-logs (Figs. 2, 15). The anatomy of the Xianchuan River section and review of previous findings from regional subsurface studies demonstrate a clear periodicity and rhythmicity of lake-basin changes during accumulation of the Yanchang Formation. Overall, the formation records the evolution of a large lake basin from inception, to growth, to repeated expansion and contraction, to final infilling (Fig. 15). The early episode of development of the Yanchang Formation was characterized by significant topographic elevation difference from the basin margin to its centre, and by an abundant sediment supply, which resulted in the development and accumulation of major large-scaled meandering and braided river systems. The Chang 9 interval was a period of lake transgression when the lake basin underwent initial expansion. The Chang 8 interval experienced a marked fluvial progradation in response to a lowered lake level at which time a major fluvio-deltaic system prograded substantially into the basin-centre lake system. The Chang 7 interval witnessed a second, more widespread lake transgression and the growth of the lake to its maximum extent, thereby enabling the accumulation and preservation of organic rich oil shale that acts as an important source rock. The Chang 6 interval records

another episode of lake regression and fluvio-deltaic progradation. The Chang 5 and 4 intervals record notable lake transgression. The Chang 3 and 2 intervals record a final lake regression and substantial fluvio-deltaic development. Following a final minor and localized lake transgression, the lake basin became filled to a point whereby minor meandering fluvial systems filled much of the remaining accommodation. Exploration efforts reveal that high-quality source rocks were developed during the Chang 7 and 9 stages when the lake expanded, whereas river-delta progradation was intense during the Chang 6, 8, 3, 2 and 10 stages when the lake regressed, preserving these successions as important reservoirs.

The four major fluvio-lacustrine transgressive-regressive cycles recorded in the Yanchang Formation were likely driven by multiple external parameters: tectonics, climate change and variations in rates of sediment delivery. Together, these factors influenced both lake level and the rate at which the lake became infilled. During the Mesozoic, the basin developed in an intracratonic setting (Liu et al, 2008). The late Triassic records the climax of the main orogenic episode in the evolution of the Qinling Mountains that bordered the southern margin of the Ordos Basin (Zhang et al, 2004; Li et al, 2007; Dong et al, 2011; Bao et al, 2014). Northward compression of the Qinling Orogen in the late Triassic is thought to have occurred as a series of pulses that drove cyclic subsidence of the southern part of the Ordos Basin and also delivered an abundant supply of clastic detritus to the subsiding basin as a response to each uplift episode (Liu, 1998, 2000; Yang, 2004; Li et al, 2007; Liu et al, 2008; Deng et al, 2013). The multiple tuff interlayers identified within the Yanchang Formation demonstrate that volcanic activity occurring in the Qinling region was contemporaneous with on-going basin subsidence and sedimentation (Zhang et al, 2009; Qiu et al, 2013).

Climate changes influenced both regional precipitation and rates of fluvial discharge; together these factors governed both lake level and the rate of fluvio-deltaic progradation. During the Chang 9 and 7 stages, the climate was humid (Zhang et al, 2007; Fan et al, 2012). Heightened precipitation and fluvial discharge resulted in lake expansion within the basin. The transgression and regression of the lake level controlled the manner by which fluvio-deltaic sand bodies became stacked. The Chang 9 and 7 intervals record episodes of higher lake level, and these intervals correspond to retrogradational styles of deltaic

sand-body stacking. By contrast, the Chang 8 and 6 intervals correspond to episodes of reduced lake level and associated accelerated rates of fluvio-deltaic progradation, thereby accounting for the dominance of sand-prone fluvio-deltaic deposits in these intervals.

The implications of steadily falling lake level on the long-term preservation potential of the fluvio-deltaic deposits that were prograding out from the basin margin are worthy of further consideration. In response to a lake-level fall, fluvial systems will potentially respond by down-cutting to reach the new lowered base level. As such, they might be expected to scour into and partly erode previously deposited fluvio-lacustrine sand bodies. However, this need not necessarily always be the case. For predominantly shallow-water lake systems with low-gradient lake beds, a lowering of lake level by even a modest amount can be expected to result in a significant dislocation of the palaeo-lake shoreline towards the centre of the basin. However, this need not necessarily result in incision: for such low-gradient systems, lowering of lake level may extend the equilibrium fluvial profile but need not necessarily steepen it, but rather is merely extend it (Emery and Myers,1996).

5.2 Characteristics of shallow-water lacustrine deltaic deposits

Shallow-water deltas in lake basins have been the subject of considerable study in recent years (Keighley et al, 2003; Keighley and Flint, 2008; Olariu et al, 2006, 2010; Turner and Tester, 2006; Zou et al, 2010). The Ordos Basin is commonly cited as an example of a shallow-water deltaic system (Zou et al, 2010; Deng et al, 2013). Many authors argue that shallow-water delta front successions are prominently characterized by subaqueous distributary-channel elements and it is these bodies that preferentially accumulate and become preserved over more out-board (i.e. seaward or lakeward) elements such as mouth bars. Thus, it is distributary-channel elements that tend to be preserved as the major sand bodies, whereas mouth bars are usually incompletely preserved and poorly expressed in stratigraphic sections as incomplete upward coarsening vertical facies successions (Mei and Lin, 1991; Lu et al, 1999; Zhu et al, 2008). However, based on observations from the Xianchuan river sections and other outcrops of the Ordos Basin (Jiao et al, 1995; Zhao et al, 2014), deltaic deposits of this system comprise both subaqueous distributary channel elements and delta-front sand bodies such as mouth-bar , distal-bar and sand-sheet elements

(Fig. 16). The type and association of preserved subaqueous deltaic sand bodies relate to their distance to the river estuary, the depth of the lake-basin water body (and its rate and sign of on-going change at the time of sedimentation), the gradient of the lake floor over which the deltaic lake-edge system prograded, and the rate of progradation.

Outcrop and seismic data from multiple studies demonstrate the existence of progradational configurations of most delta-front bodies, whether in marine or lake basins (Overeem et al, 2003; Olariu and Bhattacharya, 2006; Olariu et al, 2010; Turner and Tester, 2006; Jacob et al, 2010; Beate et al, 2010). Based on the type of basin, the gradient of the accumulation surface, and ratio between the rate of generation of accommodation via subsidence and the rate of sediment accumulation on the delta front, sand-body stacking patterns indicative of progradation can take the form of oblique, sigmoid and low-angle shingled arrangements (Berg, 1982; George, 1990). In the Chang 9, 8 and 7 intervals of the studied sections, which are exposed in sections parallel to the inferred direction of outbuilding, progradational sand-body configurations are not obvious, nor are “classic” clinof orm geometries recognized in other outcrops of the Ordos Basin (Jiao et al, 1995; Zhao et al, 2014). This is to be expected in large intracratonic lake basin succession like that of the Yanchang Formation in the Ordos Basin. Rivers debouched into the interior-draining lake basin from multiple entry points via low-gradient fluvial plains. In sub-humid climatic settings, fluvial sediments carried by freshwater flows into shallow-water lakes that themselves are also characterised by freshwater tend to form an effluent plume via a hypopycnal flow that distributes the sediment load over a broad area within the receiving lake basin. As a consequence, subaqueous distributary channels, mouth bars and distal bars tend to develop over widespread areas in such lakes, and with variable orientations (Fig. 16). The operation of these processes gives rise to important relationships: (i) deposition occurs over a wide area at any given time and in a variety of directions; (ii) the resultant gradient of the developing delta front is low such that classic clinof orm geometries may not be evident; (iii) the rate of progradation in shallow-water lake bodies is potentially very high, especially in interior draining lakes for which there is considerable run-off of sediment laden flows emanating from large catchments. Thus, progradational configurations at the delta front do not necessarily manifest themselves obviously or simply in outcrop successions.

6 Conclusions

A clear correlation exists between the sedimentary architecture revealed by this outcrop-based study and the general large-scale anatomy of the fluvio-lacustrine Yanchang Formation revealed by analysis of subsurface well-log and core data derived from boreholes spread over a wide part of the Ordos Basin. Evolution of the Yanchang Formation exhibited distinct periodicity and rhythmicity such that the 10 recognized intervals of the Yanchang Formation (Chang 10 to Chang 1) record 4 major transgressive-regressive cycles. The preserved sedimentary expression of these cycles can be identified over a series outcrop sections distributed along an 80 km-long transect. The Chang 9, 7, 4+5 and lower part of Chang 1 intervals record 4 major lacustrine transgressive events, whereas the Chang 10, 8, 6, 3 and 2 intervals record 4 major progradational events. The rhythmic evolution of the succession arose in response to systematic changes in rates of tectonic subsidence, sediment supply and changes in climate. Among these factors, tectonic subsidence was controlled by intracontinental orogenic activity in the Qinling Orogen that bordered the southern Ordos Basin.

In contrast to more commonly recognized continental shelf-edge delta systems, subaqueous distributary channels in this large, shallow-water lacustrine delta are widely developed and tend to form elongate bodies that extend continuously over tens of kilometres and accumulate several metres of channelized deposits. Such bodies are typically associated with thin-bedded mouth bar and subaqueous inter-distributary bay deposition. Generally, there is an upward-coarsening succession in the studied sections. However, the progradational architecture of the delta front is difficult to recognize in outcrop because of the low-angle trajectory of progradation into the large but shallowly dipping intracratonic Ordos Basin.

Acknowledgements

This study was supported by National Natural Science Foundation of China (Grant Nos. 41330315 and 41002071) and Opening Foundation of State Key Laboratory of Continental Dynamics, Northwest University (Grant No. BJ12146). Mounney is grateful to Areva, BHPBilliton, ConocoPhillips, Nexen, Saudi Aramco, Shell, Tullow Oil, Woodside and YPF for supporting the FRG-ERG research programme at the University of Leeds.

References

Ahmed, S., Bhattacharya, J.P., Garza, D.E., Li, Y., 2014. Facies architecture and stratigraphic evolution of a river-dominated delta front, Turonian Ferron Sandstone, Utah, U.S.A. *Journal of Sedimentary Research*, 84, 97–121.

Allen, J.R.L., 1970. Studies in fluvial sedimentation: A comparison of fining-upwards cyclothems, with special reference to coarse-member composition and interpretation. *Journal of Sedimentary Petrology* 40, 2S8–323.

Bao, C., Chen, Y., Li, D., Wang, S., 2014. Provenances of the Mesozoic sediments in the Ordos Basin and implications for collision between the North China Craton (NCC) and the South China Craton (SCC). *Journal of Asian Earth Sciences* 96, 296–307.

Beate, L.S., Leren, J., Howell, H.E., Allard, W. M., 2010. Controls on stratigraphic architecture in contemporaneous delta systems from the Eocene Roda Sandstone, Tremp–Graus basin, northern Spain. *Sedimentary Geology* 229, 9–40.

Berg, O.R., 1982. Seismic detection and evaluation of delta and turbidite sequence: their application to the exploration for the subtle trap. *The American Association of Petroleum Geologists Bulletin* 66 (9), 57–75.

Bhattacharya, J. P., 2006. Deltas. In: *Facies Models Revisited* (Eds R.G. Walker and H. Posamentier), *SEPM Spec. Publ.*, 84, 237 – 292.

Bouma, A.H., 2000. Coarse-grained and fine grained turbidite systems as end member models: Applicability and dangers. *Petroleum Geology* 17 (1), 137–143.

Bridge, J. S., 2006. Fluvial facies models: Recent developments. In: *Facies Models Revisited* (Eds R.G. Walker and H. Posamentier), *SEPM Spec. Publ.* 84, 85–170.

Carroll, A.R., Bohacs, K.M., 1999. Stratigraphic classification of ancient lakes; balancing tectonics and climatic controls. *Geology* 27, 99–102.

Coleman, J.M., Prior, D.B., 1982. Deltaic environments of deposition. *Sandstone depositional environments*. *AAPG Memoir* 31, 139–178.

Colombera, L., Mountney, N.P. and McCaffrey, W.D., 2012. A relational database for the digitization of fluvial architecture: concepts and example applications. *Petroleum Geoscience* 18, 129–140.

Colombera, L., Mountney, N.P. and McCaffrey, W.D., 2013. A quantitative approach to fluvial facies models: methods and example results. *Sedimentology* 60, 1526–1558.

Davies, N.S., Gibling, M.R., 2010a. Cambrian to Devonian evolution of alluvial systems: the sedimentological impact of the earliest land plants. *Earth Science Reviews* 98, 171–200.

Davies, N.S., Gibling, M.R., 2010b. Paleozoic vegetation and the Siluro–Devonian rise of fluvial lateral accretion sets. *Geology* 38, 51–54.

Deng, X., Fu, J., Yao, J., Pang, J., Sun, B., 2011. Sedimentary facies of the Middle–Upper Triassic Yanchang Formation in Ordos basin and breakthrough in petroleum exploration. *Journal of Palaeogeography* 13(4), 443–455. (In Chinese with English abstract)

Deng, X., Luo, A., Zhang, Z., Liu, X., 2013. Geochronological comparison on Indosinian tectonic

events between Qinling orogeny and Ordos basin. *Acta Sedimentologica Sinica* 31(6), 939–953. (In Chinese with English abstract)

Dill, H.G., Khishigsuren, S., Bulgamaa, J., Bolorma K., Melcher, F., 2006. Lithofacies and fluvial–lacustrine environments of the Palaeogene Sevkhuul and Ergil Members. *Geol. Mag.* 143 (2), 165–179.

Dong, Y., Zhang, G., Neubauer, F., Liu X., Genser, J., Hauzenberger, C., 2011. Tectonic evolution of the Qinling orogen, China: Review and synthesis. *Journal of Asian Earth Sciences* 41, 213–237.

Emery, D., Myers, K.J., 1996. *Sequence Stratigraphy*. Wiley–Blackwell, pp. 1–304.

Eric, M.R., 2007. Facies architecture and depositional environments of the Upper Cretaceous Kaiparowits Formation, southern Utah. *Sedimentary Geology* 197, 207–233.

Ethridge, F.G., 2011. Interpretation of ancient fluvial channel deposits: review and recommendations. In: *From river to rock record* (Eds. Davidson, K.S., Leleu, S. and North, C.P.), SEPM Special Publication 97, pp. 9–36.

Fan, Y., Qu H., Wang, H., Feng, Y., 2012. The application of trace elements analysis to identifying sedimentary media environment: a case study of Late Triassic strata in the middle part of western Ordos basin. *Geology in China* 39(2), 382–389. (In Chinese with English abstract)

Friend, P.F., Slater, M.J., Williams, R.C., 1979. Vertical and lateral building of river sandstone bodies, Ebro basin, Spain. *J. Geol. Soc. London* 146, 39–46.

Fu, J., Li, S., Liu, X., Deng, X., 2012. Sedimentary facies and its evolution of the Chang 9 interval of Upper Triassic Yanchang Formation in Ordos basin. *Journal of Palaeogeography* 14(3), 269–284. (In Chinese with English abstract)

George, P., 1990. An analysis of the variation in delta architecture. *Terra Nova* 2(2), 124–130.

Ghinassi, M., Libsekal, Y., Papini, M. and Rook, L., 2009. Palaeoenvironments of the Buia Homo site: High–resolution facies analysis and non–marine sequence stratigraphy in the Alat Formation (Pleistocene Dandiero basin, Danakil depression, Eritrea). *Palaeogeography, Palaeoclimatology, Palaeocology* 280, 415–431.

Jacob, A.C., Romans, W., Stephan, A.G., 2009. Outcrop expression of a continental–margin–scale shelf–edge delta from the Cretaceous Magallanes basin, Chile. *Journal of Sedimentary Research* 79, 523–539.

Jiao, Y., Li, S., Li, Z., Yang, S., Fu, Q., Lu, Z., 1995. Meandering river, delta systems and architectures of typical framework sandstones. Wuhan: Press of China University of Geosciences, pp. 1–32. (In Chinese with English abstract)

Jiao, Y., Yan, J., Li, S., Yang, R., Lang, F., Yang, S., 2005. Architectural units and heterogeneity of channel reservoirs in the Karamay Formation, outcrop area of Karamay oil field, Junggar basin, northwest China. *The American Association of Petroleum Geologists Bulletin* 89(4), 529–545.

Keighley, D.G. and Flint, S.S., 2008. Fluvial sandbody geometry and connectivity in the Middle Green River Formation, Nine Mile Canyon, southwestern Uinta basin. In: Longman, M.W. and Morgan, C.D. (eds), *Hydrocarbon systems and production in the Uinta basin, Utah*. Rocky Mountain Association of Geologists and Utah Geological Association Publication 37, 101–119.

Keighley, D., Flint, S., Howell, J. and Mosariello, A., 2003. Sequence stratigraphy in lacustrine basins: a model for part of the Green River Formation (Eocene), southwest Uinta basin, Utah, U.S.A. *Journal of Sedimentary Research* 73, 987–1006.

Li, S., Chu, M., Huang, J., Guo, Z., 2013. Characteristics and genetic mechanism of sandbody architecture in Chang-8 oil layer of Yanchang Formation, Ordos basin. *Acta Petrolei Sinica* 34(3), 435–444. (In Chinese with English abstract)

Li, S., Kusky, T.M., Wang, L., Lai, S., Liu, X., Dong, S., Zhao, G., 2007. Collision leading to multiple-stage large-scale extrusion in the Qinling orogen: insights from the Mianlue suture. *Gondwana Research* 12, 121–143.

Li, W., Pang, J., Cao, H., Xiao, L., Wang, R., 2009. Depositional system and paleogeographic evolution of the late Triassic Yangchang stage in Ordos basin. *Journal of Northwest University* 39, 501–506. (In Chinese with English abstract)

Liu S., 1998. The coupling mechanism of basin and orogen in the western Ordos basin and adjacent regions of China. *Journal of Asian Earth Science* 16, 369–383.

Liu, C., Zhao, H., Zhao, J., Wang, J., Zhang, D., Yang, M., 2008. Temporo-spatial coordinates of evolution of the Ordos basin and its mineralization responses. *Acta Geologica Sinica(English Edition)* 82(6), 1229–1243.

Liu, S., Yang, S., 2000. Upper Triassic–Jurassic sequence stratigraphy and its structural controls in the western Ordos basin, China. *Basin Research* 12, 1–18.

Lu, X., Li, C., Cai, X., Li, B., Zhao, H., 1999. Depositional characteristics and front facies reservoir framework model in Songliao shallow lacustrine delta. *Acta Sedimentologica Sinica* 17(4), 572–577. (In Chinese with English abstract)

Mei, Z., Lin, J., 1991. Stratigraphic pattern and character of skeletal sandbodies in lacustrine deltas. *Acta Sedimentologica Sinica* 9(4), 1–11. (In Chinese with English abstract)

Miall, A.D., 1985. Architectural element analysis: a new method of facies analysis applied to fluvial deposits. *Earth Science Reviews* 22, 261–308.

Miall, A.D., 1988a. Architectural elements and bounding surfaces in fluvial deposits, Anatomy of the Kayenta Formation (Lower Jurassic), southwest Colorado. *Sedimentary Geology* 55(3), 233–262.

Miall, A.D., 1988b. Reservoir Heterogeneities in Fluvial Sandstones: Lessons from Outcrop Studies. *The American Association of Petroleum Geologists Bulletin* 72(6), 682–697.

Miall, A.D., 2006. *The Geology of fluvial deposits*. Springer Berlin Heidelberg, New York, pp. 131–168.

Miall, A.D., 2014. *Fluvial depositional systems*. Springer Cham Heidelberg, New York, pp. 1–316.

Morris, T.H. and Richmond, D.R., 1992. A predictive model for reservoir continuity in fluvial sandstone bodies of a lacustrine deltaic system, Colton Formation, Utah, In Fouch, T.D., Nuccio, V.F. and Chidsey, T.C. Jr. (eds) *Hydrocarbon and Mineral Resources of the Uinta Basin, Utah and Colorado*. Utah Geological Association Guidebook 20, 227–236.

Morris, T.H., Richmond, D.R., Mariño, J.E., 1991. The Paleocene/Eocene Colton Formation: a fluvial-dominated lacustrine deltaic system, Roan Cliffs, Utah. *Utah Geological Association Publication*

19, 129–140.

Nichols, G.J., Fisher, J.A., 2007. Processes, facies and architecture of fluvial distributary system deposits. *Sedimentary Geology* 195, 75–90.

Olariu, C., Bhattacharya, J.P., 2006. Terminal distributary channels and delta front architecture of fluvial dominated delta systems. *Journal of Sedimentary Research* 76, 212–233.

Olariu, C., Steel, R.J., Petter, A.L., 2010. Delta–front hyperpycnal bed geometry and implications for reservoir modeling: Cretaceous Panther Tongue delta, Book Cliffs, Utah. *The American Association of Petroleum Geologists Bulletin* 94(6), 819–845.

Olsen, T., 1995. Fluvial and fluvio–lacustrine facies and depositional environments of the Maastrichtian to Paleocene north Horn I Formation, Price Canyon, Utah. *The Mountain Geologist* 32(2):27–44.

Overeem, I., Kroonenberg, S.B., Veldkamp, A., Groenesteijn, K., Rusakov, G.V., Svitoch, A.A., 2003. Small–scale stratigraphy in a large ramp delta: recent and Holocene sedimentation in the Volga delta, Caspian Sea. *Sedimentary Geology* 159, 133 – 157.

Qi, Y., Zhang, Z., Zhou, M., Zheng, W., 2009. Lithofacies and Sedimentary Facies from middle Triassic fluvial deposits of Youfangzhuang Formation, Jiyuan Area, western Henan. *Acta Sedimentologica Sinica* 27(2), 254–264. (In Chinese with English abstract)

Qiu, X., Liu, C., Mao, G., Deng, Yu., Wang, F., Wang, J., 2014. Late Triassic tuff intervals in the Ordos Basin, Central China: their epositional, petrographic, geochemical characteristics and regional implications. *Journal of Asian Earth Sciences* 80, 148–160.

Shanmugam, G., 2000. 50 Years of the turbidite paradigm (1950s–1990s): deep–water processes and facies models—a critical perspective. *Marine and Petroleum Geology* 17, 285–342.

Tanner, L.H., Lucas, S.G., 2010. Deposition and deformation of fluvial–lacustrine sediments of the Upper Triassic–Lower Jurassic Whitmore Point Member, Moenave Formation, northern Arizona. *Sedimentary Geology* 223, 180–191.

Taylor, A.W. and Ritts, B.D., 2004. Mesoscale heterogeneity of fluvial–lacustrine reservoir analogues: examples from the Eocene Green River and Colton formations, Uinta Basin, Utah, USA. *Journal of Petroleum Geology* 27, 3–26

Turner, B.R., Tester, G. N., 2006. The Table Rocks sandstone: a fluvial, friction–dominated lobate mouth bar sandbody in the Westphalian B coal measures, NE England. *Sedimentary Geology* 190, 97–119.

Walker, R.G., 1978. Facies models. *Geo. Sci. Canada Rep. Ser. 1*, 171–188.

Wang, S., 2001. Fluvial depositional systems and river pattern evolution of middle Jurassic Series, Datong basin. *Acta Sedimentologica Sinica* 19(4), 501–505. (In Chinese with English abstract)

Wang, Z., He, Z., Zhang, C., Li, S., Xu, L., 2004. Analysis on reservoir hierarchy of deltaic front outcrops –taking Tanjiahe outcrop in eastern Ordos Basin as an example. *Journal of Jiangnan Petroleum Institute* 26(3), 32–35. (In Chinese with English abstract)

Wanyan, R., Li, X., Liu, H., Wei, L., Liao, J., Huang, J., Huang, S., 2011. Depositional environment and eedimentary eystem of Chang 10 stage Yanchang Formation in the Ordos Basin. *Acta Sedimentologica Sinica* 29(6), 1105–1114. (In Chinese with English abstract)

Weissmann, G.S., Hartley, A.J., Nichols, G.J., Scuderi, L.A., Olson, M., Buehler, H., Banteah, R., 2010. Fluvial form in modern continental sedimentary basins: Distributive fluvial systems. *Geology*, 38(1), 39–42.

Xiao, X.M., Zhao, B.Q., Thu, Z.L., Song, Z.G., Wilkins, R.W.T., 2005. Upper Paleozoic petroleum system, Ordos Basin, China. *Marine and Petroleum Geology* 22, 945 – 963.

Xin, R., Liu, C., Lei, S., 1997. Depositional architecture analysis of coarse meandering rivers system—a case study on Jijialing outcrop. *Journal of Daqing Petroleum Institute* 21(3), 16–19. (In Chinese with English abstract)

Xu, A., Mu, L., Qiu, Y., 1998. Distribution pattern of OOIP and remaining mobile oil in different types of sedimentary reservoir of China. *Petroleum Exploration and development* 25(5), 41–44. (In Chinese with English abstract)

Yang, Y., 2004. Influence of Qinling orogenic movements in Indo–Chinese epoch to sedimentary characteristics of Yanchang Formation in Ordos Basin. *Coal Geology and Exploration* 32(5), 7–9. (In Chinese with English abstract)

Yang, Y., Li, W., Ma, L., 2005. Tectonic and stratigraphic controls of hydrocarbon systems in the Ordos Basin: a multicycle cratonic basin in central China. *The American Association of Petroleum Geologists Bulletin* 89, 255–269.

Yu, J., Yang, Y., Du, J., 2010. Sedimentation during the transgression period in Late Triassic Yanchang Formation, Ordos Basin. *Petroleum Exploration and Development* 37(2), 181–187.

Yu, X., Li, S., 2009. The Development and hotspot problems of clastic petroleum reservoir sedimentology. *Acta Sedimentologica Sinica* 27(5), 880–895. (In Chinese with English abstract)

Yu, X., Li, S., Tan, C., Xie, J., Chen, B., Yang, F., 2013. The response of deltaic systems to climatic and hydrological changes in Daihai Lake rift basin, Inner Mongolia, northern China. *Journal of Palaeogeography* 2(1), 41–55.

Zhang, G.W., Dong, Y.P., Lai, S.C., 2004. Mianlue tectonic zone and Mianlue suture zone on southern margin of Qinling–Dabie orogenic belt. *Science in China (Series D)* 47, 300–316.

Zhang, W., Yang, H., Fu, S., Zan, C., 2007. On the development mechanism of the lacustrine high–grade oil source rocks of Chang 9₁ member in Ordos the basin. *Science in China* 37, 33–38.

Zhang, W., Yang, H., Peng, P., Yang, Y., Zhang, H., Shi, X., 2009. The influence of late Triassic volcanism in the development of Chang 7 high grade hydrocarbon source rock in the Ordos Basin. *Geochimica* 38(6), 573–582.

Zhang, X., Luo, P., Gu, J., Luo, Z., Liu, L., Chen, F., 2006. Establishment of the delta sandbody framework model in the third order base level cycle: taking Ansai delta outcrop as an example. *Acta Sedimentologica Sinica* 24(4), 540–548. (In Chinese with English abstract)

Zhao, J., Liu, C., Wang, X., Zhang, C., 2009. Migration of depocenters and accumulation centers and its indication of subsidence centers in the Mesozoic Ordos Basin. *Acta Geologica Sinica (English Edition)* 83 (2), 278–294.

Zhao, J., Qu, H., Lin, J., Liu, X., Yang, Y., Lin C., 2014. Outcrop Based Anatomy of a Lacustrine Delta Succession: a Case Study from Peizhuang Section, Ordos Basin. *Acta Sedimentologica Sinica* 32(6), 9–17.

(In Chinese with English abstract)

Zhao, W., Wang, H., Yuan, X., Wang, Z., Zhu, G., 2010. Petroleum systems of Chinese nonmarine basins. *Basin Research* 22, 4–16.

Zhu, W., Li J., Zhou, X., Guo, Y., 2008. Neogene shallow–water deltaic system and large hydrocarbon accumulations in Bohai Bay, China. *Acta Sedimentologica Sinica*, 26(4):575–582. (In Chinese with English abstract)

Zou, C., Wang, L., Li, Y., Tao, S., Hou, L., 2012. Deep–lacustrine transformation of sandy debrites into turbidites, Upper Triassic, Central China. *Sedimentary Geology* 265–266, 143–155.

Zou, C., Zhang, X., Luo, P., Wang, L., Luo, Z., Liu, L., 2010. Shallow–lacustrine sand–rich deltaic depositional cycles and sequence stratigraphy of the Upper Triassic Yanchang Formation, Ordos Basin, China. *Basin Research* 22, 108–125.

Table Captions

Table 1. Summary of the characteristic features of lithofacies types encountered in the Yanchang Formation.

Table 2. Classification of architectural elements encountered in the Yanchang Formation.

Figure Captions

Figure 1. Map showing the location of the study area. a) Digital elevation map of China and the location of the Ordos Basin. b) Geological map of the Ordos Basin with the location of the basin cross-section and study area shown. c) Geological profile of the southern Ordos Basin along an east-west orientation. d) Location of the studied sites where the principal surveyed sections discussed in this paper are located.

Figure 2. a) Simplified stratigraphy of the Ordos Basin. b) Stratigraphic subdivision of the Yanchang Formation in the south-eastern part of the Ordos Basin.

Figure 3. Palaeogeographic and isopach map of the Upper Triassic Yanchang Formation in the Ordos Basin.

Figure 4. Typical facies expression in the Chang 10 interval of the Yanchang Formation. a) Outcrop photomosaic. b) Architectural relationships of lithofacies with interpretation of architectural elements. Detailed sedimentary structure: 1, 2 – medium-scale trough cross-bedding and deformed bedding; 3 – vertical succession in the middle part of measured section; 4 – mud pebbles deposited along an erosional bounding surface; 5 – preserved plant remains on bedding surfaces: woody debris and leaf impressions; 6 – trough-shaped erosional surface and associated in-fill structure; 7, 8 – trough cross-bedding and parallel bedding in channel-fill sandstone. See Figure 1 for location.

Figure 5. Typical facies association in the Chang 9 interval of the Yanchang Formation. a, b) Outcrop photomosaic. c) Architectural relationships of lithofacies with interpretation of architectural elements. Detailed sedimentary structure: 1 – low-angle trough cross-bedding; 2 – large-scale trough cross-bedding

and deformed bedding; 3, 4 – deformation structures in mouth-bar sandstone; 5 – parallel bedding and trough cross-bedding in a subaqueous distributary channel; 6 – plant fragments in dark mudstone; 7 – black shale deposited in prodelta or deep or distal lacustrine environment. See Figure 1 for location.

Figure 6. The third coarsening-upward cycle of measured section in the Chang 9 interval, Ordos Basin. See Figure 1 for location.

Figure 7. Typical facies association in the Chang 8 interval of the Yanchang Formation taken from eastern panel of Yichuan county town section. a) Outcrop photomosaic. b) Architectural relationships of lithofacies with interpretation of architectural elements. Detailed sedimentary structure: 1, 2 – preserved plant remains on bedding surface; 3 – detailed view of the section, arrow points to the convex lenticular mouth bar ; 4 – planar cross-bedding in a thick sandstone bed in the upper part of the interval; 5, 6 – small-scale ripple laminations in thin-bedded sandstone in the lower part of the Chang 8 interval. See Figure 1 for location.

Figure 8. Typical facies association in the Chang 8 interval of the Yanchang Formation taken from western panel of Yichuan county town section. a) Outcrop photomosaic. b) Architectural relationships of lithofacies with interpretation of architectural elements. Three superimposed very-thick sandstone packages are inclined down-dip toward the west. These are interpreted as the preserved record of three episodes of progradation of the delta front. Detailed sedimentary structure: 1 – large-scale trough cross-bedding structure; 2, 3 – ripple cross-lamination developed in a siltstone interlayer; 4 – interference ripple marks on a sandstone surface; 5 – sandstone beds dominate in the west (up-dip) and middle parts of measured section; 6 – trough cross-bedding with preserved woody plant debris resting on erosional surface; 7 – dark mudstone layer developed in the lower part of the section; 8 – lateral accretion surface and underlying mud bed; 9 – upward-coarsening succession developed in the eastern part of the measured section. See Figure 1 for location.

Figure 9. Typical facies association in the Chang 7 interval of the Yanchang Formation. a) Outcrop photomosaic. b) Architectural relationships of lithofacies with interpretation of architectural elements. See Figure 1 for location.

Figure 10. Typical facies association in the Chang 6 interval of the Yanchang Formation. a) Outcrop photomosaic. b) Architectural relationships of lithofacies with interpretation of architectural elements. See Figure 1 for location.

Figure 11. Typical sedimentary structures developed in the Yanchang Formation: 1 – oil shale unit developed in the Chang 7 interval. 2 – trough cross-bedding and parallel bedding developed in the Chang 6 interval; 3 – low-angle cross bedding developed in the Chang 4 and 5 intervals; 4 – in-situ tree stump in sandstone beds in the Chang 4 and 5 intervals; 5 – preserved tree trunks and associated plant debris on sandstone bedding surface in the Chang 4 and 5 interval; 6 – current lineation structure on sandstone surface accompanied with parallel bedding developed in the Chang 3 interval; 7 – grey-green sandstone and underlying muddy gravel lag deposits developed in the Chang 3 interval; 9 – large-scale trough cross-bedding and parallel bedding developed in the Chang 2 interval.

Figure 12. Typical facies association in the Chang 4 and 5 interval of the Yanchang Formation based on outcrop photomosaic. See Figure 1 for location.

Figure 13. Typical facies association in the Chang 2 interval of the Yanchang Formation based on outcrop photomosaic. See Figure 1 for location.

Figure 14. Typical facies association in the Chang 1 interval of the Yanchang Formation. a) Outcrop photomosaic. b) Architectural relationships of lithofacies with interpretation of architectural elements. Detailed sedimentary structure: 1 – lateral accretion sand bodies in the western part of measured section; 2 – small-scale ripple lamination; 3 – mud pebbles deposited along an erosional bounding surface; 4 – trough cross-bedding and erosional bounding surface developed at the base of a point-bar sandstone; 5 – mud drape on lateral accretion bounding surface; 6 – asymmetrical ripple marks; 7 – preserved tree trunks in mudstone; 8 – climbing-ripple lamination; 9 – low-angle ripple lamination; 10 – thin coal bed developed in a fine-grained succession in the upper most part of the interval; 11 – ferrous concretion on siltstone surface. See Figure 1 for location.

Figure 15. Regional cross section based on borehole data showing facies distribution and evolution of the Upper Triassic Yanchang Formation, Ordos Basin. See Figure 3 for location of the section. See Figure 3 for location.

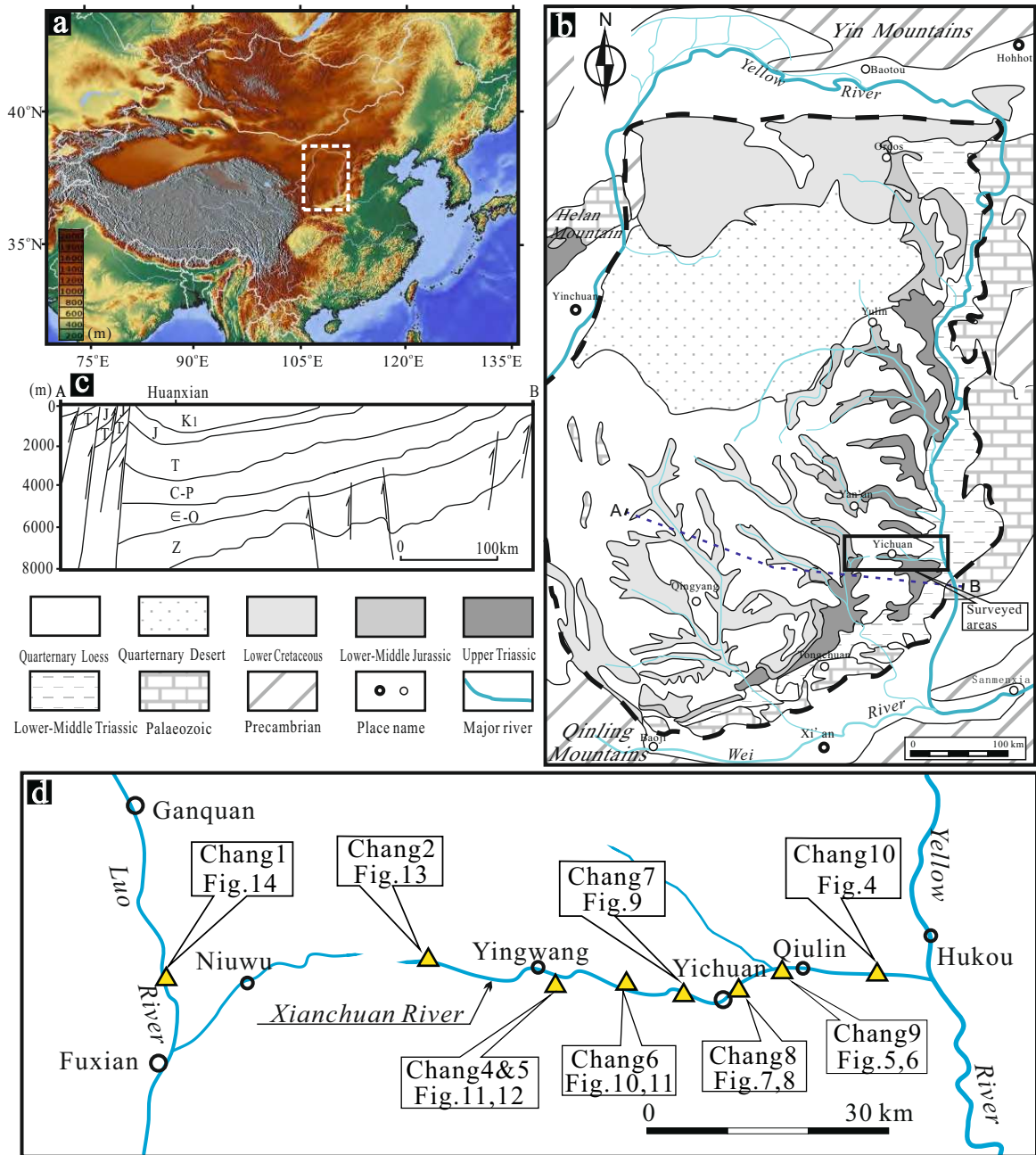
Figure 16. Model depicting the typical organization of shallow-water fluvio-deltaic facies in the Yanchang Formation. Representative vertical sections are shown: a) upward-coarsening succession recording a vertical transition from pro-delta, to delta front, to delta plain; b) proximal delta-front succession; c) distal delta-front succession. DCH – Distributary Channel; CS – Crevasse Splay; LV – Levee; LK – Small Floodplain Lake; SW – Swamp; SCH – Subaqueous Distributary Channel; SDB – Subaqueous Distributary Bay; MB – Mouth Bar; DB – Distal Mouth Bar; SB – Sheet-like Bar; PD- Prodelta.

Table 1. Summary of the characteristic features of the lithofacies types encountered in the Yanchang Formation.

<i>Code</i>	<i>Lithology</i>	<i>Sedimentary structure</i>	Interpretation
Sm	Fine- to medium-grained sandstone; sage green, yellow-green or flesh red	Massive, structureless	Rapid, in-channel deposition, mainly as scour fill
St	Fine- to medium-grained sandstone; sage green, yellow-green	Medium to large scale trough cross-bedded; extra-clasts at base; rarely deformed	Lower flow regime; sets <0.3 m thick represent 3D mesoforms (dunes); sets >0.3 m thick represent macroforms (bars) with curved or sinuous crest lines
Sp	Fine- to medium-grained sandstone; sage green, yellow-green	Medium to large scale planar cross-bedded	Lower flow regime; sets <0.3 m thick represent 2D mesoforms (dunes); sets >0.3 m thick represent macroforms (bars) with straight crest lines
Sl	Fine- to medium-grained sandstone; sage green, yellow-green	<10°inclined planar foresets	Upper flow regime; primary current lineation
Fr	Siltstone and silty claystone	Ripple cross-laminated; small-scale cross-bedded	2D and 3D current and wave ripples
Fh	Siltstone and silty claystone	Horizontally bedded	Overbank deposition; waning-stage flood deposits; subaqueous suspension fallout
Fw	Interbedded siltstone and claystone	Wavy, lenticular or flaser lamination and cross-lamination	Alternating energy regimes; typical of wave action in shoreline and near-shore setting
Fm	Siltstone and claystone	Massive; structureless	Overbank or drape deposits; subaqueous suspension fallout
C	Thin coal bed	Laminated, commonly clay-prone and platy	Frequent flooding of coal swamp

Table 2. Classification of architectural elements encountered in the Yanchang Formation.

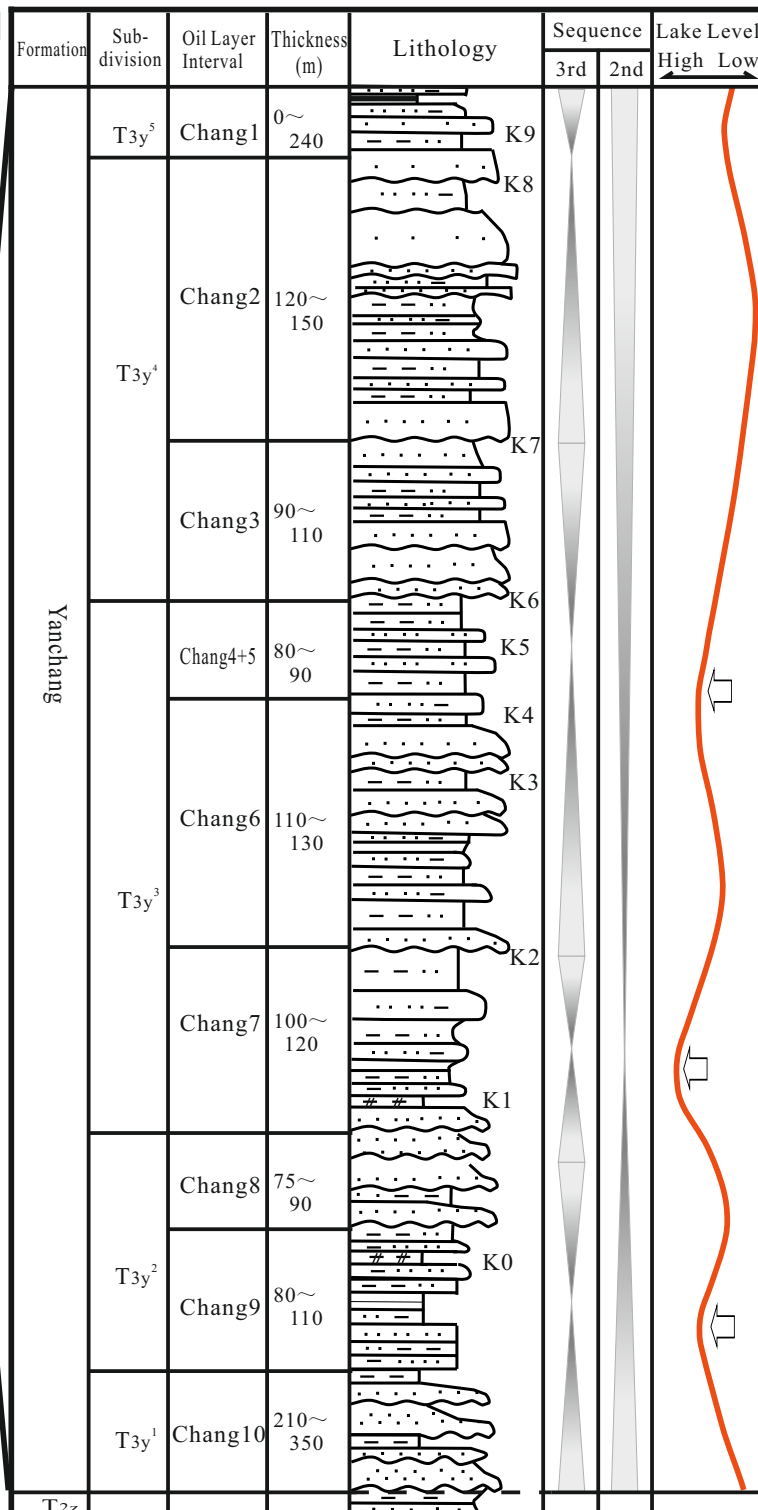
<i>Sedimentary environment</i>	<i>architectural element type</i>	<i>Code</i>	<i>Characteristic lithofacies, notable features and relationships</i>	Intervals in which recognised
Meandering river	Channel	CH	Lithofacies: Sc, St, Sl, Sp. Basal surface erosional with 0.2–0.5 m of incision; composed internally of LA elements; common overall upward-fining trend; sand bodies typically have lenticular geometries.	Chang10, Chang1
	Lateral accretion	LA	Lithofacies: Sc, St, Sl, Sp. Lenticular-shaped bodies, laterally juxtaposed to form the main part of the fill of CH elements.	Chang1
	Crevasse splay	CS	Lithofacies: Sm, Sh, St, Sr, Fl, Fm. Poorly sorted, lobes and lenticular sheet like bodies	Chang10, Chang1
	Levee	LV	Lithofacies: Fl, Fr, commonly with desiccation cracks; sheet- or wedge-shaped bodies.	Chang10, Chang1
	Floodplain fine	FF	Lithofacies: intercalations of Fl, Fm, commonly in the form of siltstone-mudstone couplets; sheet like or irregular tabular bodies	Chang10, Chang1
	Swamp	SW	Lithofacies: C alternating with Fl, Fm. Occur as thin bodies nested within FF elements.	Chang1
Subaqueous delta	Subaqueous Channel	SCH	Lithofacies: Sc, St, Sp, Sl. Moderate to slight erosion on basal surfaces; commonly associated with mud-pebble lag deposits; may occur as several juxtaposed sand bodies.	Chang9, Chang8, Chang6, Chang3, Chang2
	Subaqueous Distributary Bay	SDB	Lithofacies: Fh, Fm. Sheet- or wedge-like, fine-grained body; commonly intimately associated with SCH.	Chang9, Chang8, Chang6
	Mouth bar	MB	Lithofacies: Fr, Fl, Sp. Lenticular sand body with sharp but flat basal surface and convex-up upper surface.	Chang8
	Distal mouth bar	DB	Lithofacies: Fr, Fl. Syn-depositional deformation structures are common; sheet- or wedge-shaped body; distal part of MB.	Chang8
	Sheet-like bar	SB	Lithofacies: Fr, Fl. Sheet-like body; re-deposited sand from MB	Chang8
	Pro-delta	PD	Lithofacies: Fm, Fl. Deposited below wave base, fish and bivalve fossils common.	Chang9, Chang7
Shallow Lake	Shallow Lake Sand beach	SSB	Lithofacies: Fr, Fl, Fw, St. sheet-like bodies interbedded with thin layers of mudstone.	Chang4+5
	Shallow Lake Sand ridge	SSR	Lithofacies: Fr, Fl, Sp, St. Striped sand body with sharp but flat basal surface and convex-up upper surface.	Chang4+5

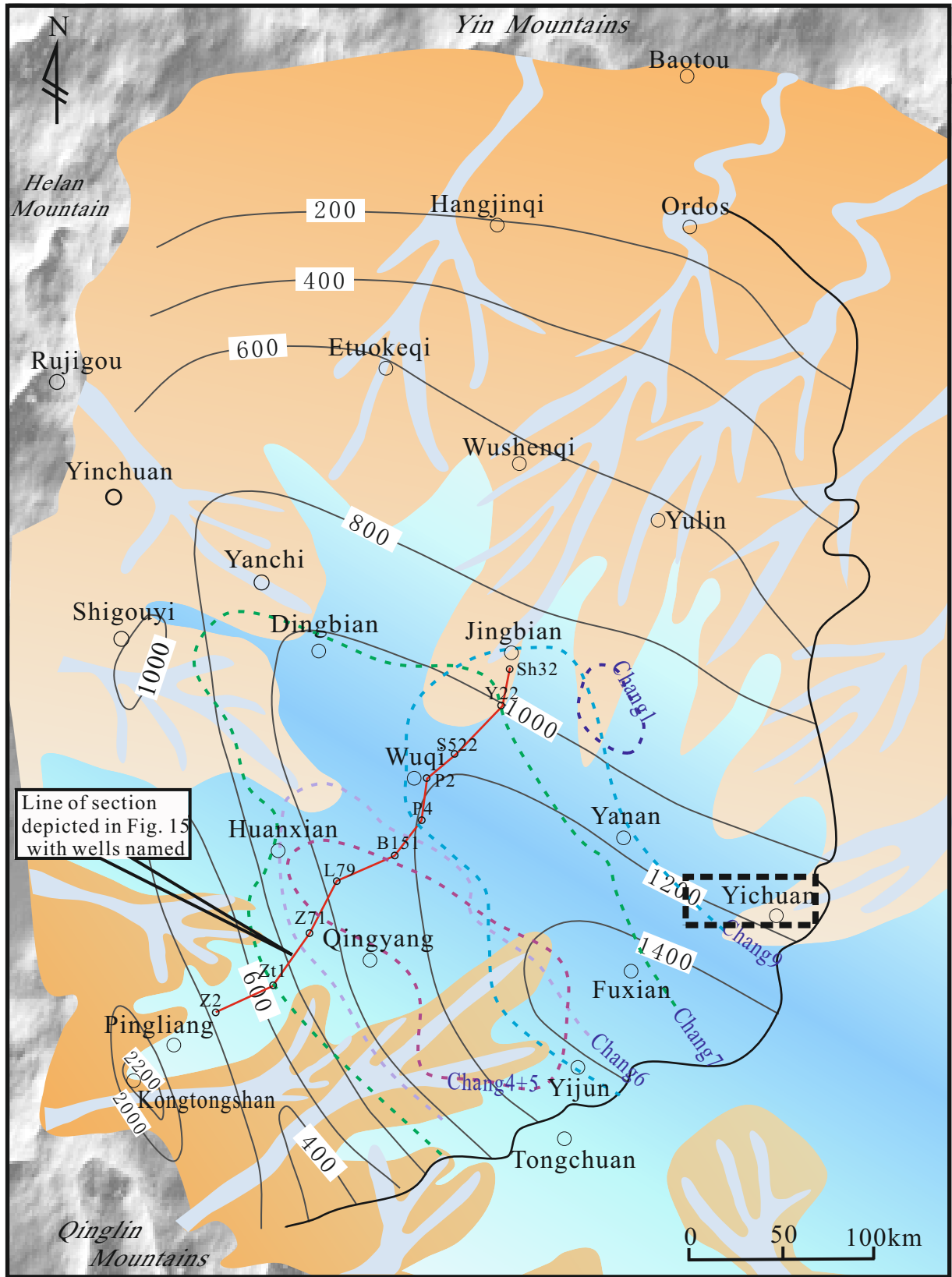


a

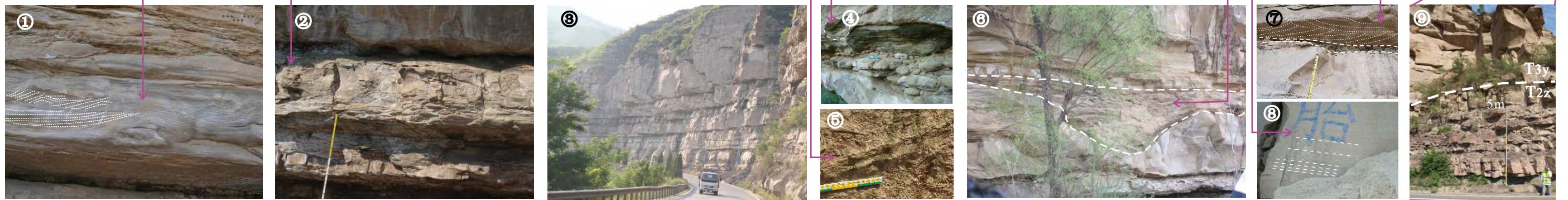
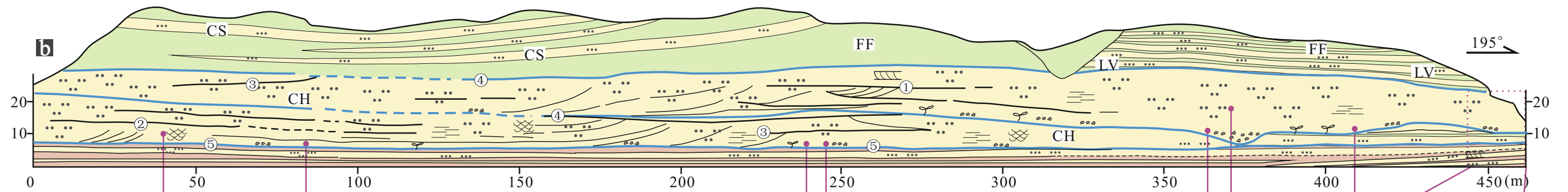
Stratigraphy		Thickness (m)	Lithology
Age	Formation/Group		
Upper Neogene-Quaternary		20-80	
		40-80	
Upper Cretaceous-Lower Neogene			No preservation
Lower Cretaceous	Zhidian Group (K _{1zh})	Jingchuan	
		Luohandong	
		Huanhe	
		Huachi	
		Luohe	
Yijun			
Upper Jurassic	Fenfanghe (J _{3f})	0-1100	
Lower-Middle Jurassic	Anding (J _{2a})	100-250	
	Zhiluo (J _{2z})	150-400	
	Yan'an (J _{2y})	150-350	
	Fuxian (J _{1f})	50-140	
Middle-Upper Triassic	Yanchang (T _{3y})	400-1300	
	Zhifang (T _{2z})	300-350	
Middle Carboniferous-Middle Triassic		1200-2000	

Conglomerate	Sandstone	Siltstone	Mudstone
Shale	Oil shale	Marlstone	Limestone
Coal	Red Clay	Loess	Unconformity
Discontinuity	Marker bed	Major transgression	

b



					
deltaic-lacustrine system	Residual extent of Yanchang Fm.	Isobath of the Yanchang Fm. (metres)	Limit of deep lacustrine facies for various Chang intervals	Place name or well name	Surveyed sections in this study



- | | | | | | | | | | | | |
|------------------|--------------------------|--------------------------|-------------------------|--------------------------|------------|--------------|-----------|-------------------|----------------------|----------------------|-----------------------|
| | | | | | | | | | | | |
| Pebbly sandstone | Coarse-grained sandstone | Medium-grained sandstone | Fine-grained sandstone | Siltstone | Mudstone | Shale | Coal Seam | Tuff | Trough cross-bedding | Planar cross-bedding | Horizontal lamination |
| | | | | | | | | | | | |
| Parallel bedding | Ripple lamination | Convolute bedding | Symmetrical ripple mark | Asymmetrical ripple mark | Mud cracks | Lag deposits | Nodule | Erosional surface | Bivalves | Log imprints | Plant fragment |

